

# Robust Stabilization and PID Control for Nonlinear Discretized Systems on a Grid Pattern

Yoshifumi Okuyama

**Abstract**—This paper describes robust stabilization and PID control for discrete-time and discrete-value (discretized/quantized) control systems. Although all control systems are currently realized using discretized signals, the analysis and design of such nonlinear discrete-time control systems has not been elucidated. In this paper, the robust stability analysis of discrete-time and discrete-value (digital) control systems with discretizing units at the input and output sides of a nonlinear continuous element (sensor/actuator) are examined in a frequency domain, and a method of designing PID control and robust stabilization for nonlinear discretized systems on a grid pattern in the time and control variables space is presented. A modified Nichols diagram and parameter specifications are used in this study. Numerical examples are provided to verify the validity of the designing method.

## I. INTRODUCTION

Currently, almost all feedback control systems are realized using discretized (discrete-time and discrete-value, i.e., digital) signals. However, the analysis and design of discretized/quantized control systems has not been entirely elucidated. The first attempt to elucidate the problem was described in a paper by Kalman [1] in 1956. Since then, many researchers have studied this problem, particularly the aspect of understanding and mitigating the quantization effects in quantized feedback control, e.g., [2], [3], [4]. However, few results have been obtained for the stability analysis of the nonlinear discrete-time feedback system.

This paper describes the robust stability analysis of discrete-time and discrete-value control systems and presents a method for designing (stabilizing) PID control for nonlinear discretized systems. The PID control scheme has been widely used in practice and theory thus far irrespective of whether it is continuous or discrete in time [5], [6] since it is a basic feedback control technique.

In the previous study [7], a robust stability condition for nonlinear discretized control systems that accompany discretizing units (quantizers) at equal spaces was examined in a frequency domain. It was assumed that the discretization is executed at the input and output sides of a nonlinear continuous element (sensor/actuator) and that the sampling period is chosen such that the size is suitable for discretization in the space. This paper presents a designing problem for discretized control systems on a grid pattern in the time and controller variables space. In this study, the concept of modified Nyquist and Nichols diagrams for nonlinear control

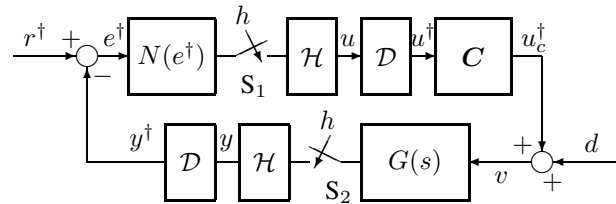


Fig. 1. Nonlinear sampled-data PID control system.

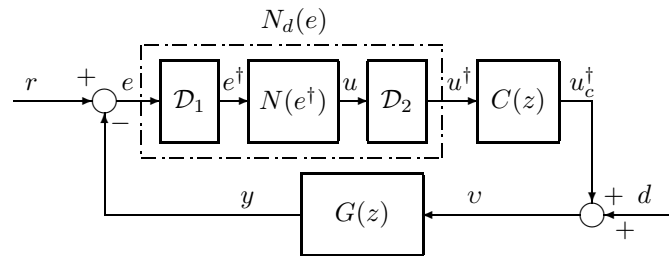


Fig. 2. Discretized nonlinear PID control system.

systems given in [8], [9] is applied to the designing procedure in the frequency domain.

## II. DISCRETIZED CONTROL SYSTEM

The discretized control system in question is represented by a sampled-data (discrete-time) feedback system with two samplers,  $S_1$  and  $S_2$ , as shown in Fig. 1. In the figure,  $\mathcal{D}$  and  $\mathcal{H}$  denote the discretizing and the zero-order holding units, respectively, which are usually performed in A/D (D/A) conversion. Moreover,  $N(\cdot)$ ,  $C$ , and  $G(s)$  are a nonlinear continuous element, a digital controller (compensator) based on the PID control scheme, and a linear continuous plant (physical system to be controlled), respectively.

When the two samplers operate synchronously with a sampling period  $h$ , the nonlinear sampled-data control system can be transformed into a discrete-time control system as shown in Fig. 2. Here,  $G(z)$  is the  $z$ -transform of  $G(s)$  together with the zero-order hold,  $C(z)$  is the  $z$ -transform of the digital PID controller  $C$ , and  $\mathcal{D}_1$  and  $\mathcal{D}_2$  are the discretizing units at the input and output sides of the nonlinear element, respectively. The relationship between  $e$  and  $u^dagger = N_d(e)$  is a stepwise nonlinear characteristic on a grid pattern as shown in Fig. 3. In this paper, a round-down discretization, which is usually executed on a computer, is applied. Therefore, the relationship between  $e^dagger$  and  $u^dagger$  is indicated by small circles on the stepwise nonlinear characteristic.

Yoshifumi Okuyama is a director of Humanitech Laboratory Co., Ltd., 115-7, Nakatsuura, Hachiman-cho, Tokushima, 770-8072, Japan oku@humanitech-lab.jp

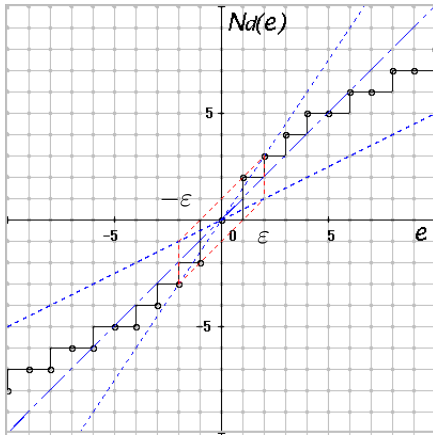


Fig. 3. Discretized nonlinear characteristics on a grid pattern.

In Figs. 1 and 2, each symbol  $e, u, y, \dots$  indicates the sequence  $e(k), u(k), y(k), \dots, (k = 0, 1, 2, \dots)$  in discrete time, but for continuous value. Each symbol  $e^\dagger, u^\dagger, \dots$  indicates a discrete value that can be assigned to an integer number, e.g.,

$$e^\dagger \in \{\dots, -3\gamma, -2\gamma, -\gamma, 0, \gamma, 2\gamma, 3\gamma, \dots\},$$

$$u^\dagger \in \{\dots, -3\gamma, -2\gamma, -\gamma, 0, \gamma, 2\gamma, 3\gamma, \dots\},$$

where  $\gamma$  is the resolution of each variable ( $\gamma > 0$ ). In the above expression, it is assumed that the input and output signals of the nonlinear characteristic have the same resolution in the discretization. Here,  $e^\dagger$  and  $u^\dagger$  also represent the sequence  $e^\dagger(k)$  and  $u^\dagger(k)$ . Without loss of generality, hereafter, we assume  $\gamma = 1.0$ .

On the other hand, the time variable  $t$  is defined as

$$t \in \{0, h, 2h, 3h, \dots\}$$

for the sampling period  $h$ . In other words, the following integer time sequence is defined:

$$k \in Z_+, \quad Z_+ = \{0, 1, 2, 3, \dots\}.$$

That is, the variables  $e^\dagger(k), u^\dagger(k),$  and  $u_c^\dagger(k)$  are defined on a grid pattern that is composed of integers in the time and controller variables space.

In this paper, the stepwise nonlinear characteristic for the controller, as shown in Fig. 3,

$$N_d(e) = Ke + g(e), \quad 0 < K < \infty, \quad (1)$$

is partitioned into the following two sections:

$$|g(e)| \leq \bar{g} < \infty, \quad (2)$$

for  $|e| < \varepsilon$ , and

$$|g(e)| \leq \beta |e|, \quad 0 \leq \beta < \infty, \quad (3)$$

for  $|e| \geq \varepsilon$ . Equation (2) represents a bounded nonlinear characteristic that exists in a finite region. On the other hand, equation (3) represents a sectorial nonlinearity for which the equivalent linear gain exists in a limited range. When considering the robust stability in a global sense, it is sufficient to consider the nonlinear term (3) for  $|e| \geq \varepsilon$

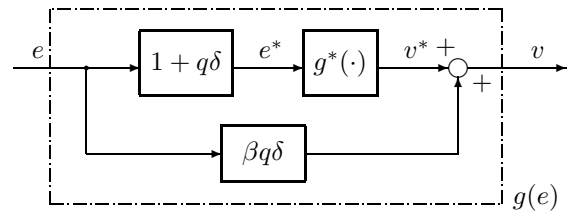


Fig. 4. Nonlinear subsystem.

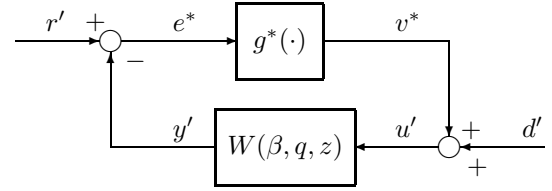


Fig. 5. Equivalent feedback system.

because the nonlinear term (2) can be treated as a disturbance signal [7]. (In this study, a fluctuation or an offset of error is assumed to be allowable in  $|e| < \varepsilon$ .)

### III. EQUIVALENT DISCRETE-TIME SYSTEM

Based on the above consideration, the following new sequences  $e_m^{*\dagger}(k)$  and  $v_m^{*\dagger}(k)$  are defined:

$$e_m^{*\dagger}(k) = e_m^\dagger(k) + q \cdot \frac{\Delta e^\dagger(k)}{h}, \quad (4)$$

$$v_m^{*\dagger}(k) = v_m^\dagger(k) - \beta q \cdot \frac{\Delta e^\dagger(k)}{h}. \quad (5)$$

where  $q$  is a non-negative number,  $e_m^\dagger(k)$  and  $v_m^\dagger(k)$  are neutral points of sequences  $e^\dagger(k)$  and  $v^\dagger(k)$ , and  $\Delta e^\dagger(k)$  is the backward difference of sequence  $e^\dagger(k)$ . The relationship between equations (4) and (5) with respect to the continuous values is shown by the block diagram in Fig. 4. In this figure,  $\delta$  is defined as

$$\delta(z) := \frac{2}{h} \cdot \frac{1 - z^{-1}}{1 + z^{-1}}. \quad (6)$$

Thus, the loop transfer function from  $v^*$  to  $e^*$  can be given by  $W(\beta, q, z)$ , as shown in Fig. 5, where

$$W(\beta, q, z) = \frac{(1 + q\delta(z))G(z)C(z)}{1 + (K + \beta q\delta(z))G(z)C(z)}, \quad (7)$$

and  $r', d'$  are transformed exogenous inputs. Here, the variables such as  $v^*, u'$  and  $y'$  written in Fig. 5 indicate the  $z$ -transformed ones.

In this paper, the following assumption is provided on the basis of the relatively fast sampling and the slow response of the controlled system.

**[Assumption]** The absolute value of the backward difference of sequence  $e(k)$  does not exceed  $\gamma$ , i.e.,

$$|\Delta e(k)| = |e(k) - e(k-1)| \leq \gamma. \quad (8)$$

If condition (8) is satisfied,  $\Delta e^\dagger(k)$  is exactly  $\pm\gamma$  or 0 because of the discretization. That is, the absolute value of the backward difference can be given as

$$|\Delta e^\dagger(k)| = |e^\dagger(k) - e^\dagger(k-1)| = \gamma \text{ or } 0. \quad \square$$

The assumption stated above will be satisfied by the following examples. The phase trace of backward difference  $\Delta e^\dagger$  is shown in the figure.

#### IV. NORM INEQUALITIES

In this section, some lemmas with respect to an  $\ell_2$  norm of the sequences are presented. Here, we define a new nonlinear function

$$f(e) := g(e) + \beta e. \quad (9)$$

When considering the discretized output of the nonlinear characteristic,  $v^\dagger = g(e^\dagger)$ , the following expression can be given:

$$f(e^\dagger(k)) = v^\dagger(k) + \beta e^\dagger(k). \quad (10)$$

From inequality (3), it can be seen that the function (10) belongs to the first and third quadrants.

When considering the equivalent linear characteristic, the following inequality can be defined:

$$0 \leq \psi(k) := \frac{f(e^\dagger(k))}{e^\dagger(k)} \leq 2\beta. \quad (11)$$

When this type of nonlinearity  $\psi(k)$  is used, inequality (3) can be expressed as

$$v^\dagger(k) = g(e^\dagger(k)) = (\psi(k) - \beta)e^\dagger(k). \quad (12)$$

For the neutral points of  $e^\dagger(k)$  and  $v^\dagger(k)$ , the following expression is given from (10):

$$\frac{1}{2}(f(e^\dagger(k)) + f(e^\dagger(k-1))) = v_m^\dagger(k) + \beta e_m^\dagger(k). \quad (13)$$

Moreover, equation (12) is rewritten as

$$v_m^\dagger(k) = (\psi(k) - \beta)e_m^\dagger(k).$$

Since  $|e_m^\dagger(k)| \leq |e_m(k)|$ , the following inequality is satisfied when a round-down discretization is executed:

$$|v_m^\dagger(k)| \leq \beta |e_m^\dagger(k)| \leq \beta |e_m(k)|. \quad (14)$$

Based on the above premise, the following norm conditions are examined [7].

**[Lemma-1]** The following inequality holds for a positive integer  $p$ :

$$\|v_m^\dagger(k)\|_{2,p} \leq \beta \|e_m^\dagger(k)\|_{2,p} \leq \beta \|e_m(k)\|_{2,p}. \quad (15)$$

Here,  $\|\cdot\|_{2,p}$  denotes the Euclidean norm, which can be defined by

$$\|x(k)\|_{2,p} := \left( \sum_{k=1}^p x^2(k) \right)^{1/2}.$$

(Proof) The proof is clear from inequality (14).  $\square$

**[Lemma-2]** If the following inequality is satisfied with respect to the inner product of the neutral points of (10) and the backward difference:

$$\langle v_m^\dagger(k) + \beta e_m^\dagger(k), \Delta e^\dagger(k) \rangle_p \geq 0, \quad (16)$$

the following inequality can be obtained:

$$\|v_m^{*\dagger}(k)\|_{2,p} \leq \beta \|e_m^{*\dagger}(k)\|_{2,p} \quad (17)$$

for any  $q \geq 0$ . Here,  $\langle \cdot, \cdot \rangle_p$  denotes the inner product, which is defined as

$$\langle x_1(k), x_2(k) \rangle_p = \sum_{k=1}^p x_1(k)x_2(k).$$

(Proof) The following equation is obtained from (4) and (5):

$$\begin{aligned} & \beta^2 \|e_m^{*\dagger}(k)\|_{2,p}^2 - \|v_m^{*\dagger}(k)\|_{2,p}^2 \\ &= \beta^2 \|e_m^\dagger(k)\|_{2,p}^2 - \|v_m^\dagger(k)\|_{2,p}^2 \\ &+ \frac{2\beta q}{h} \cdot \langle v_m^\dagger(k) + \beta e_m^\dagger(k), \Delta e^\dagger(k) \rangle_p. \end{aligned} \quad (18)$$

Thus, (17) is satisfied by using the left inequality of (15). Moreover, as for the input of  $g^*(\cdot)$ , the following inequality can be obtained from (18) and the right inequality (15):

$$\|v_m^{*\dagger}(k)\|_{2,p} \leq \beta \|e_m^*(k)\|_{2,p}. \quad (19)$$

$\square$

The left side of inequality (16) can be expressed as a sum of trapezoidal areas.

**[Lemma-3]** For any step  $p$ , the following equation is satisfied:

$$\begin{aligned} \sigma(p) &:= \langle v_m^\dagger(k) + \beta e_m^\dagger(k), \Delta e^\dagger(k) \rangle_p \\ &= \frac{1}{2} \sum_{k=1}^p (f(e^\dagger(k)) + f(e^\dagger(k-1))) \Delta e^\dagger(k). \end{aligned} \quad (20)$$

(Proof) The proof is clear from (13).

In general, the sum of trapezoidal areas holds the following property.

**[Lemma-4]** If inequality (8) is satisfied with respect to the discretization of the control system, the sum of trapezoidal areas becomes non-negative for any  $p$ , that is,

$$\sigma(p) \geq 0. \quad (21)$$

(Proof) The proof was presented in [7].  $\square$

#### V. ROBUST STABILITY IN A GLOBAL SENSE

By applying a small gain theorem to the loop transfer characteristic (7), the following robust stability condition of the discretized nonlinear control system can be derived [7].

**[Theorem]** If there exists a  $q \geq 0$  in which the sector parameter  $\beta$  with respect to nonlinear term  $g(\cdot)$  satisfies the following inequality, the discrete-time control system with sector nonlinearity (3) is robust stable in an  $\ell_2$  sense:

$$\beta < \beta_0 = K\eta(q_0, \omega_0) = \max_q \min_\omega K\eta(q, \omega), \quad (22)$$

when the linearized system with nominal gain  $K$  is stable.

The  $\eta$ -function is written as follows:

$$\begin{aligned} \eta(q, \omega) &:= \\ &= \frac{-q\Omega \sin \theta + \sqrt{q^2\Omega^2 \sin^2 \theta + \rho^2 + 2\rho \cos \theta + 1}}{\rho}, \end{aligned} \quad (23)$$

$$\forall \omega \in [0, \omega_c],$$

where  $\Omega(\omega)$  is the distorted frequency of angular frequency  $\omega$  and is given by

$$\delta(e^{j\omega h}) = j\Omega(\omega) = j\frac{2}{h} \tan\left(\frac{\omega h}{2}\right), \quad j = \sqrt{-1} \quad (24)$$

and  $\omega_c$  is a cut-off frequency. In addition,  $\rho(\omega)$  and  $\theta(\omega)$  are the absolute value and the phase angle of  $KG(e^{j\omega h})C(e^{j\omega h})$ , respectively.

(Proof) Based on the loop characteristic in Fig. 5, the following inequality can be given with respect to  $z = e^{j\omega h}$ :

$$\|e_m^*(z)\|_{2,p} \leq c_1 \|r'_m(z)\|_{2,p} + c_2 \|d'_m(z)\|_{2,p} + \sup_{z=1} |W(\beta, q, z)| \cdot \|w_m^{\dagger}(z)\|_{2,p}. \quad (25)$$

Here,  $r'_m(z)$  and  $d'_m(z)$  denote the  $z$ -transformation for the neutral points of sequences  $r'(k)$  and  $d'(k)$ , respectively. Moreover,  $c_1$  and  $c_2$  are positive constants.

By applying inequality (19), the following expression is obtained:

$$\left(1 - \beta \cdot \sup_{z=1} |W(\beta, q, z)|\right) \|e_m^*(z)\|_{2,p} \leq c_1 \|r'_m(z)\|_{2,p} + c_2 \|d'_m(z)\|_{2,p}. \quad (26)$$

Therefore, if the following inequality (i.e., the small gain theorem with respect to  $\ell_2$  gains) is valid,

$$|W(\beta, q, e^{j\omega h})| = \left| \frac{(1 + jq\Omega(\omega))\rho(\omega)e^{j\theta(\omega)}}{K + (K + j\beta q\Omega(\omega))\rho(\omega)e^{j\theta(\omega)}} \right| < \frac{1}{\beta}. \quad (27)$$

the sequences  $e_m^*(k)$ ,  $e_m(k)$ ,  $e(k)$  and  $y(k)$  in the feedback system are restricted in finite values when exogenous inputs  $r(k)$ ,  $d(k)$  are finite and  $p \rightarrow \infty$ . From the square of both sides of inequality (27), (22) is given.  $\square$

## VI. MODIFIED NICHOLS DIAGRAM

In the previous papers [8], [9], the inverse function was used instead of the  $\eta$ -function, i.e.,  $\xi(q, \omega) = \frac{1}{\eta(q, \omega)}$ . Using the notation, inequality (22) can be rewritten as follows:

$$M_0 = \xi(q_0, \omega_0) = \min_q \max_\omega \xi(q, \omega) < \frac{K}{\beta}. \quad (28)$$

When  $q = 0$ , the  $\xi$ -function can be expressed as:

$$\xi(0, \omega) = \frac{\rho}{\sqrt{\rho^2 + 2\rho \cos \theta + 1}} = |T(e^{j\omega h})|, \quad (29)$$

where  $T(z)$  is the complementary sensitivity function for the discrete-time system.

It is evident that the following curve on the gain-phase plane,

$$\xi(0, \omega) = M, \quad (M : \text{const.}) \quad (30)$$

corresponds to the contour of the constant  $M$  in the Nichols diagram. In this study, since an arbitrary non-negative number  $q$  is considered, the  $\xi$ -function that corresponds to (29) and (30) is given as follows:

$$\frac{\rho}{-q\Omega \sin \theta + \sqrt{q^2\Omega^2 \sin^2 \theta + \rho^2 + 2\rho \cos \theta + 1}} = M. \quad (31)$$

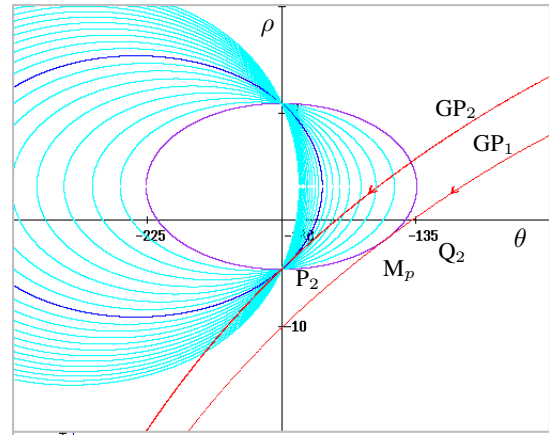


Fig. 6. Modified contours and gain-phase curves ( $M = 1.4$ ,  $c_q = 0.0, \dots, 4.0$ ).

From this expression, the following quadratic equation can be obtained:

$$(M^2 - 1)\rho^2 + 2\rho M(M \cos \theta - q\Omega \sin \theta) + M^2 = 0. \quad (32)$$

The solution of this equation is expressed as follows:

$$\rho = -\frac{M}{M^2 - 1}(M \cos \theta - q\Omega \sin \theta) \pm \frac{M}{M^2 - 1} \sqrt{(M \cos \theta - q\Omega \sin \theta)^2 - (M^2 - 1)}. \quad (33)$$

The modified contour in the gain-phase plane ( $\theta, \rho$ ) is drawn based on the equation of (33). Although the distorted frequency  $\Omega$  is a function of  $\omega$ , the term  $q\Omega = c_q \geq 0$  is assumed to be a constant parameter. This assumption for  $M$  contours was also discussed in [9]. Figure 6 shows an example of the modified Nichols diagram for  $c_q \geq 0$  and  $M = 1.4$ . Here,  $GP_1$  is a gain-phase curve that touches an  $M$  contour at the peak value ( $M_p = \xi(0, \omega_p) = 1.4$ ). On the other hand,  $GP_2$  is a gain-phase curve that crosses the  $\theta = -180^\circ$  line and all the  $M$  contours at the gain crossover point  $P_2$ . That is, the gain margin  $g_M$  becomes equal to  $-20 \log_{10} M/(M + 1) = 4.68[\text{dB}]$ . The latter case corresponds to the discrete-time system in which Aizerman's conjecture is valid. At the continuous saddle point  $P_2$ , the following equation is satisfied:

$$\left(\frac{\partial \xi(q, \omega)}{\partial q}\right)_{q=q_0, \omega=\omega_0} = 0. \quad (34)$$

Evidently, the phase margin  $p_M$  is obtained from the phase crossover point  $Q_2$ .

## VII. CONTROLLER DESIGN

The PID controller  $C$  applied in this study is given by the following algorithm:

$$u_c(k) = K_p u^\dagger(k) + C_i \sum_{j=0}^k u^\dagger(j) + C_d \Delta u^\dagger(k), \quad (35)$$

where  $\Delta u^\dagger(k) = u^\dagger(k) - u^\dagger(k-1)$  is a backward difference in integer numbers, and each coefficient is defined as

$$K_p, C_i, C_d \in \mathbb{Z}_+, \quad \mathbb{Z}_+ = \{0, 1, 2, 3, \dots\}.$$

Here,  $K_p$ ,  $C_i$ , and  $C_d$  correspond to  $K_p$ ,  $K_p h/T_I$ , and  $K_p T_D/h$  in the following (discrete-time  $z$ -transform expression) PID algorithm:

$$C(z) = K_p \left( 1 + \frac{h}{T_I(1-z^{-1})} + \frac{T_D}{h}(1-z^{-1}) \right). \quad (36)$$

We use algorithm (35) without division because the variables  $u^\dagger$ ,  $u_c$ , and coefficients  $K_p$ ,  $C_i$ ,  $C_d$  are integers.

Using the  $z$ -transform expression, equation (35) is written as:

$$\begin{aligned} u_c(z) &= C(z)u(z) \\ &= (K_p + C_i(1+z^{-1}+z^{-2}+\dots) + C_d(1-z^{-1}))u(z). \end{aligned}$$

In the closed form, controller  $C(z)$  can be given as

$$C(z) = K_p + C_i \cdot \frac{1}{1-z^{-1}} + C_d(1-z^{-1}) \quad (37)$$

for discrete-time systems. When comparing equations (36) and (37),  $C_i$  and  $C_d$  become equal to  $K_p h/T_I$  and  $K_p T_D/h$ , respectively.

The design method adopted in this paper is based on the classical parameter specifications in the modified Nichols diagram. This method can be conveniently designed, and it is significant in a physical sense (i.e., mechanical vibration and resonance).

### VIII. NUMERICAL EXAMPLES

**[Example-1]** Consider the following controlled system:

$$G(s) = \frac{K_1}{(s+0.04)(s+0.2)(s+0.4)}, \quad (38)$$

where  $K_1 = 0.0001 = 1.0 \times 10^{-4}$ . The discretized nonlinear characteristic (discretized sigmoid, i.e. arc tangent [10]) is as shown in Fig. 3. Here, the resolution value is  $\gamma = 1$  as described in section 2. For C-language expression, it can be written as

$$\begin{aligned} e^\dagger &= \gamma * (\text{double})(\text{int})(e/\gamma) \\ u &= 0.4 * e^\dagger + 3.0 * \text{atan}(0.6 * e^\dagger) \\ u^\dagger &= \gamma * (\text{double})(\text{int})(u/\gamma), \end{aligned}$$

where (int) and (double) denote the conversion into an integral number (a round-down discretization) and the re-conversion into a double-precision real number, respectively.

In this paper, the sampling period is chosen as a base unit  $h = 1$ . When choosing the nominal gain  $K = 1.0$  and the threshold  $\varepsilon = 2.0$ , the sectorial area of the stepwise nonlinear characteristic for  $\varepsilon \leq |e|$  can be determined as

TABLE I

PID PARAMETERS FOR EXAMPLE-1 ( $g_M$ : GAIN MARGINS,  $p_M$ : PHASE MARGINS,  $M_p$ : PEAK VALUES,  $\beta_0$ : ALLOWABLE SECTORS).

	$K_p$	$C_i$	$C_d$	$\beta_0$	$g_M$ [dB]	$p_M$ [deg]	$M_p$
(i)	100	0	0	1.34	4.6	67.6	0.91
(ii)	100	2	20	1.07	13.4	56.8	1.07
(iii)	100	4	20	1.02	12.1	45.3	1.32

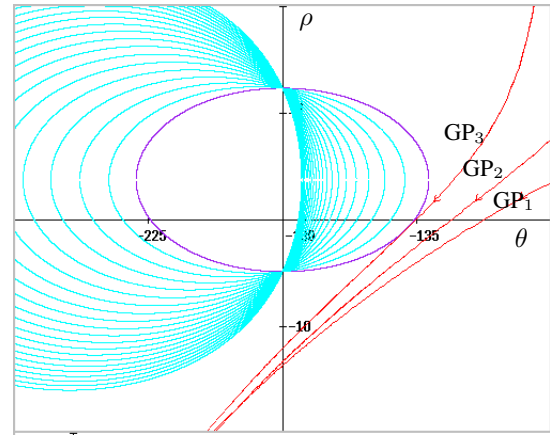


Fig. 7. Modified contours and gain-phase curves for Example-1 ( $M = 1.4$ ,  $c_q = 0.0, \dots, 4.0$ ).

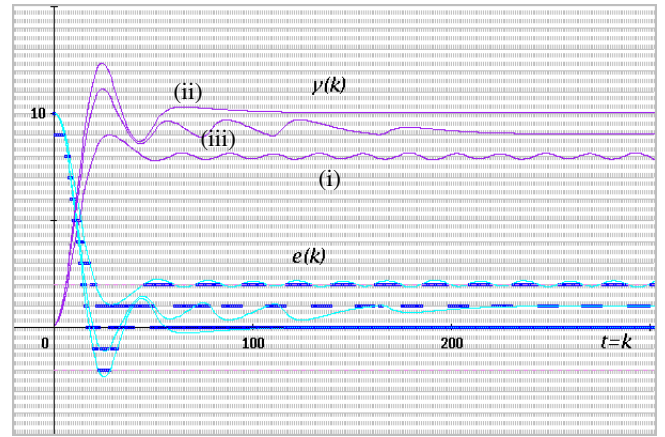


Fig. 8. Step responses for Example-1.

[0.5, 1.5] drawn by dotted lines in the figure. Fig. 7 shows gain-phase curves of  $KG(e^{j\omega h})C(e^{j\omega h})$  on the modified Nichols diagram. Here, GP<sub>1</sub>, GP<sub>2</sub>, and GP<sub>3</sub> are cases (i), (ii), and (iii), respectively. The PID parameters are specified as shown in Table I. The gain margins  $g_M$ , the phase margin  $p_M$  and the peak value  $M_p$  can be obtained from the gain crossover points  $P$ , the phase crossover points  $Q$ , and the points of contact with regard to the  $M$  contours, respectively.

The max-min value  $\beta_0$  is calculated from (22) (e.g., (i)) as follows:

$$\beta_0 = \max \eta(q, \omega_0) = \eta(q_0, \omega_0) = 0.91.$$

Therefore, the allowable sector for nonlinear characteristic  $g(\cdot)$  is given as [0.0, 1.91]. The stability of discretized control system (i) (and also systems (ii),(iii)) will be guaranteed. In this example, the continuous saddle point (34) appears (i.e., Aizerman's conjecture is satisfied). Thus, the allowable sector of equivalent gain  $K_\ell$  can be given as  $0 < K_\ell < 1.91$ .

Figure 8 shows time responses for the three cases, and Figure 9 shows phase traces. As is obvious from Fig. 9, assumption (8) is satisfied. The step response (i) remains a sustained oscillation and an off-set. However, as for (ii) and (iii) the responses are improved by using the PID, especially integral (I: a summation in this paper) algorithm.

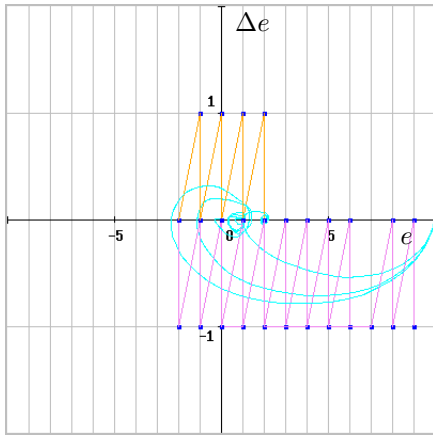


Fig. 9. Phase traces for Example-1.

TABLE II

PID PARAMETERS FOR EXAMPLE-2 ( $g_M$ : GAIN MARGINS,  $p_M$ : PHASE MARGINS,  $M_p$ : PEAK VALUES,  $\beta_0$ : ALLOWABLE SECTORS).

	$K_p$	$C_i$	$C_d$	$\beta_0$	$g_M$ [dB]	$p_M$ [deg]	$M_p$
(i)	100	0	0	0.91	15.5	40.6	1.44
(ii)	100	2	20	0.65	15.4	28.6	2.02
(iii)	100	4	20	0.46	14.4	17.1	3.36

**[Example-2]** Consider the following controlled system:

$$G(s) = \frac{K_2(s+0.2)(-s+0.4)}{(s+0.02)(s+0.04)(s+1.0)}, \quad (39)$$

where  $K_2 = 0.001 = 1.0 \times 10^{-3}$ . The same nonlinear characteristic and the nominal gain are chosen as shown in Example-1. The modified Nichols diagram with gain-phase curves of  $KG(e^{j\omega h})C(e^{j\omega h})$  is as shown in Fig. 10. Here,  $GP_1$ ,  $GP_2$  and  $GP_3$  are cases (i), (ii), and (iii), and the PID parameters are specified as shown in Table I. Figure 11 shows time responses for the three cases. In this example, although the allowable sector of equivalent linear gain (e.g., case (iii)) is  $0 < K_\ell < 4.1$ , the allowable sector for nonlinear characteristic becomes  $[0.0, 1.46]$  as shown in Table II. Since the sectorial area of the stepwise nonlinear characteristic is  $[0.5, 1.5]$ , the stability of the nonlinear control system cannot be guaranteed. The response for (iii) actually fluctuates as shown in Fig. 11. This is a counter example for Aizerman's conjecture.

## IX. CONCLUSION

In this paper, we have described robust stabilization and discretized PID control for continuous plants on a grid pattern with respect to controller variables and time elapsed. A robust stability condition for nonlinear discretized feedback systems was presented along with a method for designing PID control. The design procedure employs the modified Nichols diagram and its parameter specifications. The stability margins of the control system are specified directly in the diagram. Further, the numerical examples showed that the time responses can be stabilized for the required performance.

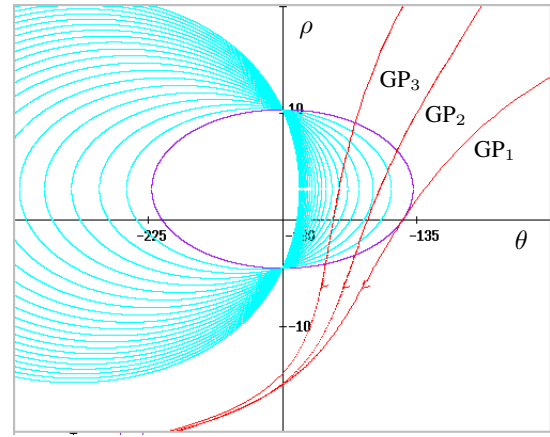


Fig. 10. Modified contours and gain-phase curves for Example-2 ( $M = 1.09$ ,  $c_q = 0.0, \dots, 4.0$ ).

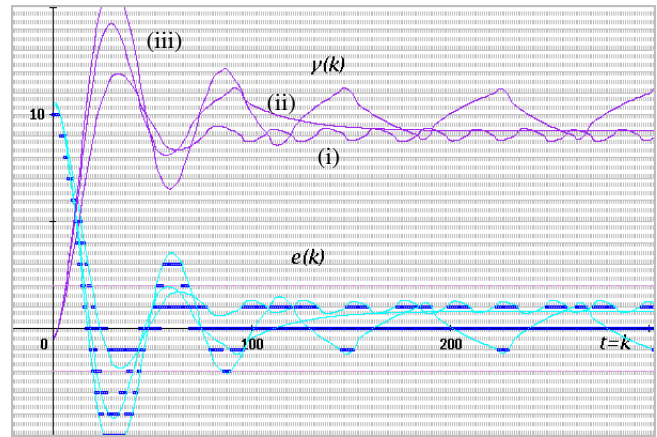


Fig. 11. Step responses for Example-2.

## REFERENCES

- [1] R. E. Kalman, "Nonlinear Aspects of Sampled-Data Control Systems", *Proc. of the Symposium on Nonlinear Circuit Analysis*, vol. VI, pp.273-313, 1956.
- [2] R. E. Curry, *Estimation and Control with Quantized Measurements*, Cambridge, MIT Press, 1970.
- [3] D. F. Delchamps, "Stabilizing a Linear System with Quantized State Feedback", *IEEE Trans. on Automatic Control*, vol. 35, pp. 916-924, 1990.
- [4] M. Fu, "Robust Stabilization of Linear Uncertain Systems via Quantized Feedback", *IEEE Int. Conf. on Decision and Control*, TuA06-5, 2003.
- [5] A. Datta, M.T. Ho and S.P. Bhattacharyya, *Structure and Synthesis of PID Controllers*, Springer-Verlag, 2000.
- [6] F. Takemori and Y. Okuyama, "Discrete-Time Model Reference Feedback and PID Control for Interval Plants" *Digital Control 2000: Past, Present and Future of PID Control*, Pergamon Press, pp. 260-265, 2000.
- [7] Y. Okuyama, "Robust Stability Analysis for Discretized Nonlinear Control Systems in a Global Sense", *Proc. of the 2006 American Control Conference*, Minneapolis, USA, pp. 2321-2326, 2006.
- [8] Y. Okuyama et al., "Robust Stability Evaluation for Sampled-Data Control Systems with a Sector Nonlinearity in a Gain-Phase Plane" *Int. J. of Robust and Nonlinear Control*, Vol. 9, No. 1, pp. 15-32, 1999.
- [9] Y. Okuyama et al., "Robust Stability Analysis for Non-Linear Sampled-Data Control Systems in a Frequency Domain", *European Journal of Control*, Vol. 8, No. 2, pp. 99-108, 2002.
- [10] Y. Okuyama et al., "Amplitude Dependent Analysis and Stabilization for Nonlinear Sampled-Data Control Systems", *Proc. of the 15th IFAC World Congress*, T-Tu-M08, 2002.